Thermal stability of amorphous $GaN_{1-x}As_x$ alloys

A. X. Levander,[1,2] Z. Liliental-Weber,[1] R. Broesler,[1,2] M. E. Hawkridge,[1] S. V. Novikov,[3] C. T. Foxon,[3] O. D. Dubon,[1,2] J. Wu,[1,2] W. Walukiewicz,[1] and K. M. Yu[1,a)]
[1]*Materials Sciences Division, Lawrence Berkeley National Laboratory, Berkeley, California 94720, USA*
[2]*Department of Materials Science and Engineering, University of California, Berkeley, California 94720, USA*
[3]*School of Physics and Astronomy, University of Nottingham, Nottingham NG7 2RD, United Kingdom*

(Received 16 January 2011; accepted 28 March 2011; published online 19 April 2011)

$GaN_{1-x}As_x$ alloys grown across the composition range by low temperature molecular beam epitaxy have great technological potential for photovoltaic applications owing to their strong absorption coefficient and wide tunability of band gap and band edges. We found that amorphous $GaN_{1-x}As_x$ alloys that are formed for the compositions x, in the range of $x \sim 0.3-0.7$ are stable up to 700 °C. This is surprising since growth of $GaN_{1-x}As_x$ above 400 °C results in phase segregation. At annealing temperatures higher than 700 °C the alloy phase segregates into GaAs:N and GaN:As. The relative size of the nanocrystals depends on the initial film composition and annealing conditions. © *2011 American Institute of Physics*. [doi:10.1063/1.3581894]

Over the past decade, it has been well established that the isoelectronic substitution of anions with very different ion size and/or electronegativity can result in dramatic restructuring of the electronic bands. These materials are difficult to synthesize due to large miscibility gaps owing to the inherent mismatch of the anion alloying elements. The resulting compounds are referred to as highly mismatched alloys (HMAs), and prominent examples include dilute As-rich and N-rich $GaN_{1-x}As_x$ and $ZnTe_{1-x}O_x$.[1–5]

We have demonstrated that the miscibility gap of the $GaN_{1-x}As_x$ system can be overcome by using low temperature molecular beam epitaxy (LT-MBE).[6–9] At low growth temperatures near ~200 °C the $GaN_{1-x}As_x$ system can be grown across the entire composition range on crystalline and amorphous substrates but for $0.10 < x < 0.75$ the resulting alloy is amorphous. The optical band gap of the $GaN_{1-x}As_x$ system covers a wide spectral range of 0.8–3.4 eV varying systematically with composition. Recently, amorphous $GaN_{1-x}Bi_x$ HMAs with up to $x \sim 0.10$ have also been synthesized by the LT-MBE method.[10] Theoretical work has predicted that amorphous GaN could be a technologically useful electronic material due to the lack of deep gap states.[11] Therefore, given the strong absorption and availability of band gap engineering over a wide range, the amorphous nitride-based HMAs could have technological potential, especially in solar energy conversion devices. In this letter we investigate the thermal stability of amorphous $GaN_{1-x}As_x$ alloys in both rapid and furnace anneals. The high temperature stability of these highly nonequilibrium alloys is important since device fabrication typically requires processing at elevated temperatures (e.g., diffusion doping, dielectric deposition, etc.).

The GaNAs films were grown on 2 in. c-plane sapphire substrates using plasma assisted MBE. The growth temperature was in the range of 200–400 °C. Further details of the growth of these amorphous alloys can be found in previous publications.[6–8] The composition and crystallinity of these films has been characterized using Rutherford backscattering spectrometry (RBS), particle induced x-ray emission, electron probe microanalysis, x-ray diffraction (XRD), and transmission electron microscopy (TEM) as reported in Refs. 6–9.

The rapid thermal annealing (RTA) process was conducted in nitrogen ambient with a GaN wafer proximity cap in the temperature range of 300–950 °C for 10–60 s. For films with low arsenic contents (<0.35) negligible composition redistribution of the Ga and As elements was observed within the resolution limit of RBS. For films with higher initial arsenic contents, more significant decomposition in the form of reduced arsenic surface concentration and reduced overall thickness was observed. For example, Fig. 1 shows the RBS spectra of a 510 nm thick $GaN_{0.43}As_{0.57}$ film before and after 850 °C 20 s RTA. The annealing process reduced the As content in the top 280 nm of the film to $x \sim 0.17$. This decomposed region was also contaminated with up to 10% residual oxygen detected using the 3.04 MeV $^{16}O(\alpha,\alpha)^{16}O$ reaction. A reduction in the overall thickness of ~15 nm is also observed.

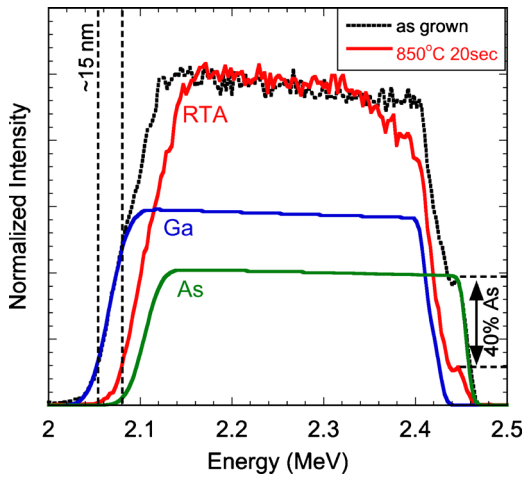

FIG. 1. (Color online) RBS spectra for as grown $GaN_{0.43}As_{0.57}$ (dashed) and 850 °C 20 s RTA $GaN_{0.43}As_{0.57}$ (solid). The simulated Ga and As contributions to the spectra are shown for the as grown sample. The RTA resulted in a reduction in As in the surface region and an overall reduction in film thickness.

a)Electronic mail: kmyu@lbl.gov.

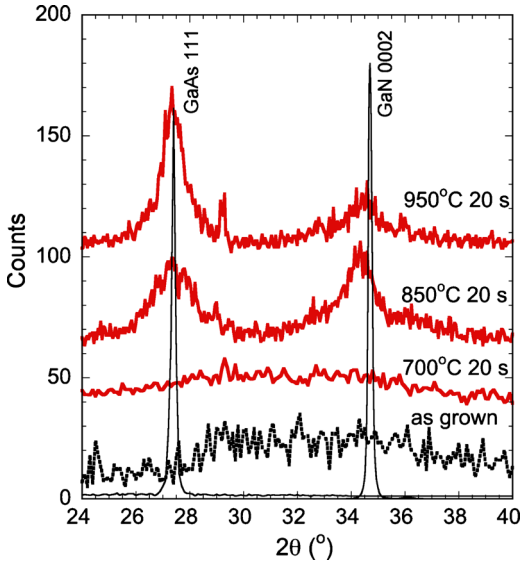

FIG. 2. (Color online) XRD patterns from a $GaN_{0.64}As_{0.36}$ film after successive RTA treatments at increasing temperature for 20 s each, with GaAs and GaN standards. The GaAs:N (111) and GaN:As (0002) peak positions indicate phase segregation of the amorphous ternary alloy into the corresponding binary crystalline phases.

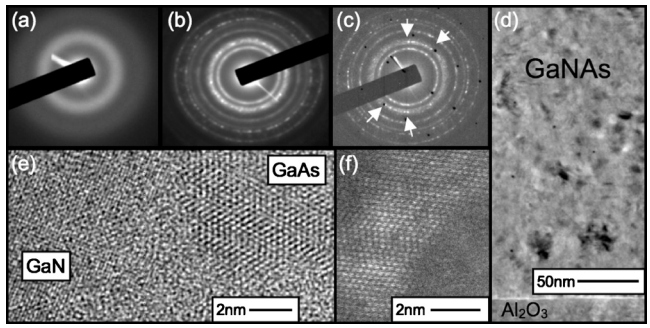

FIG. 3. SAD patterns for a-$GaN_{0.64}As_{0.36}$ as grown (a); after 850 °C 20 s RTA (b), and after 950 °C 20 s RTA taken close to the interface (c) (black spots from Al_2O_3 substrate). Note the strong dotted pattern within the second ring due to (0002) GaN planes. (d) Cross-section of the film showing the formation of randomly distributed grains. (e) High resolution image showing formation of GaAs (larger lattice spacings) and GaN (smaller lattice spacings) crystals. (f) Z-contrast microscopy image of a GaAs grain (brighter contrast from heavier As atoms). Note twinning within the GaAs crystals in (e) and (f).

The XRD patterns in Fig. 2 show the effect of RTA on the crystallinity of a $GaN_{0.64}As_{0.36}$ film. No crystalline peak can be observed for the film annealed at 700 °C for 20 s. After RTA at 850 °C both GaAs:N (111) and GaN:As (0002) diffraction peaks are present. The intensity of the two peaks was dependent on the initial film composition, with a high initial As content resulting in a more intense GaAs:N (111) peak. In low As-content films after 850 °C 20 s RTA (Fig. 2), the GaN:As peak shifts to lower angle from that of pure GaN while the GaAs:N peak shows no shift. This suggests that GaN:As is more thermally stable than GaAs:N. After annealing at higher temperatures (950 °C), the GaN:As peak agrees with pure GaN indicating further out diffusion of the remaining arsenic. The maximum As fraction in the crystalline GaN:As formed is estimated to be 3.5%. We have performed similar RTA processing on films in the range of $0.30 < x < 0.70$ and found similar behavior. The RTA results suggest that amorphous GaNAs HMA films are stable up to 700 °C for short periods, with phase segregation into GaAs:N and GaN:As occurring at around 800 °C.

Furnace anneals were conducted to determine the long-term thermal stability of the alloys. For GaNAs films with intermediate As compositions, we observed that for one hour anneals up to 600 °C in 1atm nitrogen ambient, phase segregation did not occur and the films were still amorphous. After annealing for 1 h at 700 °C the film was completely decomposed due to the high partial pressures of the anions in the GaNAs films. These results suggest that the thermal stability of a-GaNAs alloy films is exceptional considering that crystallization of ion implantation amorphized GaAs and GaN occurs at temperatures as low as 200 °C and 500 °C, respectively.[12] Moreover, for MBE growth of GaNAs alloys with As content higher than ~5%, phase segregation occurs at growth temperatures above 400 °C, but the alloys become amorphous below 400 °C.[6–8] The stability of the amorphous phase also suggests that the cations and anions in the as-grown a-GaNAs alloys are indeed randomly distributed so that long-range diffusion at higher temperatures or long time periods is needed for the kinetically driven crystallization or decomposition to occur. This randomly, homogeneously distributed cation–anion configuration may also present a thermodynamic energy barrier against phase segregation.

The average crystallite size of annealed films was estimated by analyzing the XRD diffraction patterns using the Scherrer equation. The average GaAs:N and GaN:As crystallite sizes for a $GaN_{0.64}As_{0.36}$ sample are 10.5 nm and 16 nm, respectively, after 850 °C 20 s RTA. RTA at 950 °C 20 s results in a larger GaAs:N crystal size of ~22 nm while the GaN:As grain size is unchanged. A higher arsenic content ($x \sim 0.70$) in the initial $GaN_{1-x}As_x$ film resulted in larger GaAs (29 nm) and smaller GaN (12.7 nm) grain sizes for 850 °C 20 s RTA.

The as grown films have been characterized by TEM and have been shown to have diffuse electron diffraction ring patterns and "pepper/salt" diffraction contrast on high resolution micrographs, characteristic of an amorphous material.[8,9] TEM results from a $GaN_{0.64}As_{0.36}$ sample as grown and after 850 °C 20 s RTA is shown in Figs. 3(a) and 3(b). Using Al_2O_3 as an internal standard, the interplanar distances from the selected area diffraction (SAD) pattern have been calculated. A comparison of the interplanar distances measured by SAD and XRD with the calculated powder diffraction data from GaAs and GaN is shown in Table I. The SAD pattern clearly shows both GaN:As and GaAs:N rings indicating phase segregation in the annealed sample. The first and second rings from the center correspond to the GaAs (111) plane and a superposition of the $(1\underline{1}00)$, (0002), and $(10\underline{1}1)$ planes of GaN. For a sample annealed at 950 °C, the spotty pattern from the GaN (0002) ring at a specific arc [marked by arrows in Fig. 3(c)] may suggest a preferential crystallization direction, especially close to the substrate.

Bright-field images from cross-section samples show the formation of small crystals distributed uniformly throughout the film [Fig. 3(d)]. The high-resolution image [Fig. 3(e)] taken using a JEOL CM300 Sub-Angstrom TEM with 300keV accelerating voltage shows both GaAs (larger lattice spacings) and GaN (smaller lattice spacings) nanocrystals. Using Z-contrast imaging (Philips Tecnai –300 keV) the crystals with larger lattice spacings were identified as GaAs. Some of the GaAs crystals are twinned, possibly due to ni-

TABLE I. A comparison of the interplanar distances measured by SAD and XRD for $GaN_{0.64}As_{0.36}$ after 850 °C 20 s RTA with the calculated power diffraction data from GaAs and GaN. The double arrow indicates one broad ring measured from the inner diameter, the strongly dotted pattern, and the outer diameter.

d-spacing (experimental) (Å)			Calc. powder diffraction standard	
SAD		XRD	GaN (hkl)	GaAs (hkl)
3.28		3.252		3.26 (111)
2.75			2.75 ($1\underline{1}00$)	
2.55		2.60	2.58 (0002)	
2.4			2.43 ($10\underline{1}1$)	
1.98			1.88 ($10\underline{1}2$)	1.998 (220)
1.68 (weak)				1.70 (311)
1.58			1.58 ($\underline{2}110$)	
1.47			1.46 ($10\underline{1}3$)	1.413 (400)
1.35			1.38 ($22\underline{0}0$)	1.297 (331)

trogen incorporation. Amorphouslike contrast is visible in high-resolution images suggesting the nanocrystals are embedded in an a-GaNAs matrix, although small grains not satisfying the diffraction condition may cause this contrast.

The optical band gap (E_g) of the alloys was characterized by optical absorption spectroscopy. The absorption spectra of a $GaN_{0.70}As_{0.30}$ film as grown and after 850 °C 20 s RTA shows a shift in the alloy E_g from 1.57 to 1.87 eV after RTA (Fig. 4). This suggests that after RTA, more GaAs:N than GaN:As nanocrystals are formed so that the remaining amorphous matrix has less As. From the higher E_g of the $GaN_{1-x}As_x$ alloy an As content of $x \sim 0.25$ after RTA can be estimated.[8,9] Although small GaAs:N crystals are formed after RTA, no significant absorption greater than the

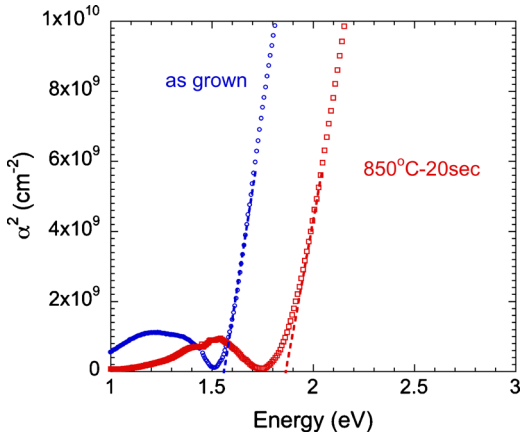

FIG. 4. (Color online) Absorption spectra from as grown and 850 °C 20 s RTA $GaN_{0.70}As_{0.30}$. The shift in the band edge indicates the formation of a higher band gap phase.

magnitude of Fabry–Perot oscillations at 1.4 eV is expected due to the relatively small volume fraction of GaAs:N. This band edge shift to higher energy after RTA was observed for GaNAs alloys with different compositions and as grown alloy E_g spanning $1.55\ \text{eV} < E_g < 2.2\ \text{eV}$.

In summary, the amorphous HMA GaNAs alloys display unexpectedly high thermal stability for long-term anneals at 600 °C. Phase segregation occurs after rapid annealing at 800 °C and above, with GaAs:N and GaN:As nanocrystals homogeneously nucleated and distributed uniformly throughout the entire film. The resulting size of the nanocrystalline GaAs:N and GaN:As was dependent on the initial film composition and RTA conditions.

This work was supported by the Director, Office of Science, Office of Basic Energy Sciences, Materials Sciences and Engineering Division, of the U.S. Department of Energy under Contract No. DE-AC02-05CH11231. The use of the National Center for Electron Microscopy at Lawrence Berkeley Laboratory is appreciated. Some of the characterization work was supported by National Science Foundation under Grant No. CBET-0932905. The growth work at the University of Nottingham was supported by the EPSRC (Grant Nos. EP/I004203/1, EP/G046867/1, and EP/G030634/1). A. Levander acknowledges the National Science Foundation for financial support.

[1]W. Walukiewicz, W. Shan, K. M. Yu, J. W. Ager III, E. E. Haller, I. Miotkowski, M. J. Seong, H. Alawadhi, and A. K. Ramdas, Phys. Rev. Lett. **85**, 1552 (2000).
[2]W. Shan, W. Walukiewicz, J. W. Ager III, E. E. Haller, J. F. Geisz, D. J. Friedman, J. M. Olson, and S. R. Kurtz, Phys. Rev. Lett. **82**, 1221 (1999).
[3]K. Uesugi, N. Morooka, and I. Suemune, Appl. Phys. Lett. **74**, 1254 (1999).
[4]J. Wu, W. Walukiewicz, K. M. Yu, J. D. Denlinger, W. Shan, J. W. Ager III, A. Kimura, H. F. Tang, and T. F. Kuech, Phys. Rev. B **70**, 115214 (2004).
[5]K. M. Yu, W. Walukiewicz, J. Wu, W. Shan, J. W. Beeman, M. A. Scarpulla, O. D. Dubon, and P. Becla, Phys. Rev. Lett. **91**, 246403 (2003).
[6]S. V. Novikov, C. R. Staddon, A. V. Akimov, R. P. Campion, N. Zainal, A. J. Kent, C. T. Foxon, C. H. Chen, K. M. Yu, and W. Walukiewicz, J. Cryst. Growth **311**, 3417 (2009).
[7]S. V. Novikov, C. R. Staddon, C. T. Foxon, K. M. Yu, R. Broesler, M. Hawkridge, Z. Liliental-Weber, W. Walukiewicz, J. Denlinger, and I. Demchenko, J. Vac. Sci. Technol. B **28**, C3B12 (2010).
[8]K. M. Yu, S. V. Novikov, R. Broesler, I. N. Demchenko, J. D. Denlinger, Z. Liliental-Weber, F. Luckert, R. W. Martin, W. Walukiewicz, and C. T. Foxon, J. Appl. Phys. **106**, 103709 (2009).
[9]K. M. Yu, S. V. Novikov, R. Broesler, Z. Liliental-Weber, A. X. Levander, V. M. Kao, O. D. Dubon, J. Wu, W. Walukiewicz, and C. T. Foxon, Appl. Phys. Lett. **97**, 101906 (2010).
[10]A. X. Levander, K. M. Yu, S. V. Novikov, A. Tseng, C. T. Foxon, O. D. Dubon, J. Wu, and W. Walukiewicz, Appl. Phys. Lett. **97**, 141919 (2010).
[11]P. Stumm and D. A. Drabold, Phys. Rev. Lett. **79**, 677 (1997).
[12]S. O. Kucheyev, J. S. Williams, and S. J. Pearton, Mater. Sci. Eng. R. **33**, 51 (2001).